A novel method produces native light-harvesting complex II aggregates from the photosynthetic membrane revealing their role in nonphotochemical quenching

Received for publication, September 25, 2020, and in revised form, October 15, 2020 Published, Papers in Press, October 20, 2020, DOI 10.1074/jbc.RA120.016181

Mahendra K. Shukla[1], **Akimasa Watanabe**[2,3], **Sam Wilson**[1], **Vasco Giovagnetti**[1], **Ece Imam Moustafa**[1], **Jun Minagawa**[2,3,*], **and Alexander V. Ruban**[1,*]

From the [1]*School of Biological and Chemical Sciences, Queen Mary University of London, London, United Kingdom, the* [2]*Division of Environmental Photobiology, National Institute for Basic Biology, Okazaki, Japan, and the* [3]*Department of Basic Biology, School of Life Science, SOKENDAI, The Graduate University for Advanced Studies, Okazaki, Japan*

Edited by Joseph M. Jez

Nonphotochemical quenching (NPQ) is a mechanism of regulating light harvesting that protects the photosynthetic apparatus from photodamage by dissipating excess absorbed excitation energy as heat. In higher plants, the major light-harvesting antenna complex (LHCII) of photosystem (PS) II is directly involved in NPQ. The aggregation of LHCII is proposed to be involved in quenching. However, the lack of success in isolating native LHCII aggregates has limited the direct interrogation of this process. The isolation of LHCII in its native state from thylakoid membranes has been problematic because of the use of detergent, which tends to dissociate loosely bound proteins, and the abundance of pigment–protein complexes (*e.g.* PSI and PSII) embedded in the photosynthetic membrane, which hinders the preparation of aggregated LHCII. Here, we used a novel purification method employing detergent and amphipols to entrap LHCII in its natural states. To enrich the photosynthetic membrane with the major LHCII, we used *Arabidopsis thaliana* plants lacking the PSII minor antenna complexes (NoM), treated with lincomycin to inhibit the synthesis of PSI and PSII core proteins. Using sucrose density gradients, we succeeded in isolating the trimeric and aggregated forms of LHCII antenna. Violaxanthin- and zeaxanthin-enriched complexes were investigated in dark-adapted, NPQ, and dark recovery states. Zeaxanthin-enriched antenna complexes showed the greatest amount of aggregated LHCII. Notably, the amount of aggregated LHCII decreased upon relaxation of NPQ. Employing this novel preparative method, we obtained a direct evidence for the role of *in vivo* LHCII aggregation in NPQ.

The photosynthetic apparatus of plants, algae, and cyanobacteria converts solar energy into chemical energy, generating most of the organic matter on Earth. Photosystem II (PSII) uses water as an unlimited source of electrons and, utilizing the energy of photons, breaks it into molecular oxygen, protons, and electrons (1). The sequestered electrons are used to reduce $NADP^+$ to NADPH, whereas the coupled translocation of protons into the thylakoid lumen drives the synthesis of ATP. Both NADPH and ATP are eventually utilized to fix CO_2 into organic molecules (1). To harvest light, PSII is connected to a peripheral antenna system consisting of major light-harvesting complexes (LHCs) (the trimeric LHCII, composed of the polypeptides Lhcb1-3) and minor LHCs (the monomeric CP24 (Lhcb6), CP26 (Lhcb5), and CP29 (Lhcb4)) (2). These LHC systems have evolved to efficiently supply energy to PSII. However, under high irradiance, LHCs capture more light energy than that effectively used by downstream metabolic processes (*e.g.* CO_2 fixation). This leads to oversaturation of the electron transport chain capacity, ultimately resulting in the damage of the PSII reaction center (RCII) and decrease of photosynthetic efficiency (3–5).

Nonphotochemical quenching (NPQ) is a key feedback process activated to minimize the buildup of excitation energy pressure in PSII by means of safe, thermal dissipation of the light energy absorbed in excess (6–8). NPQ is triggered by the formation of a pH gradient (ΔpH) across the thylakoid membrane, and its major component is termed energy-dependent quenching (qE). qE is the fastest and most effective response of plants against excess light and it is regulated by the so-called "allosteric factors," zeaxanthin and photosystem II subunit S (PsbS) (7–10). Both zeaxanthin and PsbS adjust the sensitivity of qE to ΔpH. The accumulation of zeaxanthin controls the kinetics and extent of qE by enhancing NPQ upon high light exposure while slowing its rate of recovery under low light (9). Differently, PsbS senses pH changes (10–12) and appears to work as a "quick switch" between light harvesting and dissipative states to efficiently track light intensity fluctuations (7–9). The capacity of PsbS for fast tracking of light changes has been shown to have a significant impact on plant productivity and great potential for future crop improvement (8, 13).

Although the physiological significance of qE is relatively well-understood and -accepted, the quenching site and molecular mechanism of qE are still debated. Different qE sites have been proposed, with RCIIs, major LHCII trimers, the monomeric minor antennae, and PsbS being among the candidates postulated (14–18). Currently, it is widely accepted that the qE locus is within PSII antenna complexes and not in RCIIs (7, 9, 19), with PsbS not having a direct role in the formation of the quencher (20, 21). Over the years, several studies employed genetic manipulations to generate mutants lacking specific antenna proteins (reviewed in Refs. 7–9), revealing a certain

This article contains supporting information.

* For correspondence: Alexander V. Ruban, a.ruban@qmul.ac.uk; Jun Minagawa, minagawa@nibb.ac.jp.

degree of functional redundancy when specific complexes were decreased in content or absent. Recently, using a mutant of *Arabidopsis thaliana* devoid of all minor antenna proteins (*NoM*), the presence of two antenna-based quenching sites was proposed: a fast-activated quenching component in monomeric LHCs and a slowly activated component in major LHCIIs (22). However, later studies revealed that minor antenna proteins, as well as RCIIs, are not essential to form the full extent of qE (23). Moreover, *NoM* mutants lacking RCIIs showed the same levels of qE measured in WT plants, which was inducible even in the absence of PsbS provided ΔpH was enhanced (24). These data identified the major trimeric LHCII and ΔpH as the unique and essential requirements for qE. Thus, LHCII trimers appear to possess the inherent ability to switch reversibly between the light-harvesting and protective states (24).

Another relevant issue is understanding how qE takes place *in vivo*, in the thylakoid membrane. The so-called "LHCII antenna aggregation model" (25) hypothesizes that lumen acidification causes LHCII complexes to aggregate, a process that is required to establish qE *via* conformational changes within the antenna complexes (8, 26, 27). Such a model has been supported by a number of spectroscopic, biochemical, and microscopy studies, providing solid experimental evidence for its occurrence (25, 28–30), but there has been no direct preparation of the native LHCII aggregates that correlated with the NPQ kinetics. PsbS and zeaxanthin were both found to promote aggregation of LHCII (9, 29, 31–34). PsbS was reported to interact with both major and minor LHCII proteins, with zeaxanthin synthesis modulating such interactions (32). Although zeaxanthin accumulation is not an obligatory requirement for qE formation, it has been shown to promote and sustain qE by enhancing aggregation (28, 35). Thus, both PsbS and zeaxanthin appear to facilitate the antenna aggregation process in an allosteric fashion, by increasing antenna sensitivity to protons and tuning qE efficiently to environmental light conditions.

Despite multiple studies confirming the validity of the LHCII aggregation model and its link to qE regulation, to date, no purification method is available to isolate LHCII complexes in their native aggregated state from thylakoid membranes. The isolation of LHCII aggregates can be challenging because solubilizing photosynthetic complexes with detergents impedes the isolation of large, intact pigment–protein complexes while possibly introducing non-native conformational changes to the structure of proteins (36–38). Developing a mild solubilization methodology that avoids losing weak protein interactions, as well as the formation of artifacts, would yield native antenna aggregates instrumental to test the role of the allosteric co-factors (*e.g.* xanthophylls) during LHCII aggregation. In the mid-nineties, amphipathic polymers were developed with the aim to improve the stability of solubilized membrane proteins in an aqueous buffer relative to that observed when using detergent (39). These polymers, called amphipols (APols), have a strong hydrophilic backbone that is grafted with hydrophobic side chains, thereby making them amphipathic (39–41). Although these polymers are not particularly efficient at solubilizing biological membranes, they are capable of trapping effectively solubilized membrane proteins and keeping them stable in their native conformation (42, 43). Ionic and nonionic APols have been successfully used to stabilize highly active PSII–LHCII supercomplexes of *Chlamydomonas reinhardtii* in their major organization ($C_2S_2M_2L_2$) (43), revealing high resolution structures of these supercomplexes (44–46).

Here we used a combination of mild detergent (α-DM and digitonin) and APol A8-35 (here after Apol) to isolate aggregates of the major LHCII antenna from thylakoid membranes and study their quenching properties. Because RCIIs and minor antenna complexes are not needed for qE formation (19, 23, 24), we chose to use *Arabidopsis NoM* mutants, which are enriched in LHCII trimers (22–24), and we reduced the concentration of photosystem core complexes, especially RCIIs, by treating plants with lincomycin (19, 24). Essentially, this approach provided plants almost exclusively containing LHCII antenna complexes in their thylakoid membranes. Moreover, violaxanthin- and zeaxanthin-enriched thylakoid membranes were obtained and characterized in the dark, NPQ, and dark-relaxation states to address the role of xanthophyll cycle activity on LHCII aggregates.

Results

Preparation of the photosynthetic membranes enriched in major LHCII complexes

The aim of this work was to isolate aggregated major LHCII antenna proteins from natural thylakoid membranes, *i.e.* close-to-native aggregates of LHCII, and investigate how LHCII aggregation is modulated by the presence of different xanthophyll pigments in dark and NPQ states, as well as upon recovery from quenching. To achieve this task, we generated LHCII only–containing photosynthetic membranes using *Arabidopsis NoM* mutants that were treated with lincomycin (19). The amount of RCIIs present in the *NoM* plants used in this study was strongly reduced (Fig. S1), in line with the low F_v/F_m values measured ($F_v/F_m \leq 0.2$, whereas F_v/F_m values are ~0.83 and ~0.55 in *A. thaliana* WT and *NoM* plants not treated with lincomycin, respectively) (22, 23, 47, 48).

In the thylakoid membrane, LHCII trimers appear as partially aggregated (19), with xanthophyll cycle pigments influencing LHCII organization and quenching extent (29). Here we investigated the dependence of LHCII aggregation states on (i) the content of xanthophyll pigments and (ii) NPQ formation and relaxation. To address both aspects, we prepared thylakoid membranes by isolating chloroplast from lincomycin-treated *NoM* plants that were either enriched in violaxanthin or zeaxanthin (49), and then exposed them to darkness (dark state), high light (NPQ state), and darkness subsequent to high light (recovery state). Because chloroplast preparation from *NoM* lincomycin-treated plants showed impaired recovery from quenching, we prepared chloroplasts from protoplast to investigate this condition.

Isolation of LHCII aggregates from NoM thylakoid membranes lacking PSII cores

First, we isolated LHCII antenna complexes by using detergent only (α-DM and α-DM + digitonin for 30 min) to solubilize thylakoid membranes (Fig. S2). Although we employed very low concentrations of α-DM (0.5 or 0.3%) and digitonin

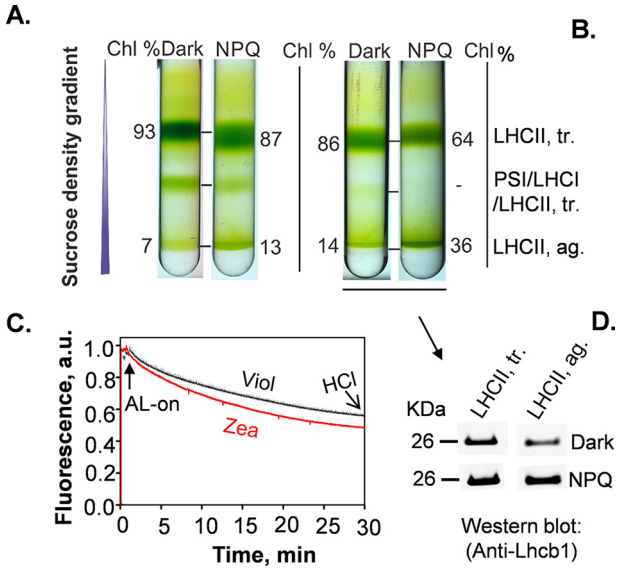

Figure 1. Purification and characterization of trimeric and aggregated forms of the major LHCII. *A* and *B*, sucrose density gradient of solubilized thylakoid membranes obtained from violaxanthin-enriched (*A*) and zeaxanthin-enriched (*B*) *NoM* plants, devoid of photosystem II and I cores by lincomycin treatment. Dark and NPQ conditions are compared. The experiments were performed on two independent replicates for violaxanthin-enriched thylakoid membranes and three replicates for zeaxanthin-enriched thylakoid membranes (Tables S2 and S3). *C*, representative chlorophyll (*Chl*) fluorescence quenching traces measured on violaxanthin-enriched (*black line*) and zeaxanthin-enriched (*red line*) chloroplasts. The *arrow* shows when actinic light was applied (*AL-on*; 1,380 μmol photons m^{-2} s^{-1}, for 30 min). NPQ state was fixed by lowering the pH from 7.6 to 5.0 units adding 2 M HCl to chloroplast suspensions. *D*, immunodetection of the LHCII trimeric (*tr.*) and aggregate (*ag.*) bands from zeaxanthin-enriched *NoM* thylakoid membrane (Fig. 1*B*) against the Lhcb1 antibody. The samples were loaded as equal volumes (20 μl). *a.u.*, arbitrary unit(s); *Viol*, violaxanthin; *Zea*, zeaxanthin.

(0.5%) during thylakoid solubilization, both procedures did not result in resolved bands of LHCII aggregates (Fig. S2). We then used a combination of detergents to solubilize the thylakoid membranes, which were subsequently replaced by APols A8–35 (1% w/v) to stabilize and isolate LHCII complexes before dissociation (41, 44) (Fig. S2). This procedure was very effective, and replacing the detergents with Apols allowed us to isolate both LHCII trimers and aggregates as discrete, resolved bands of the sucrose density gradients (Fig. S2). This procedure was therefore used to investigate the effect of NPQ, as well as xanthophylls (violaxanthin and zeaxanthin) in the formation of LHCII aggregates in *NoM* thylakoid membranes (Fig. 1). Thylakoids enriched in violaxanthin or zeaxanthin (49) were used either under dark or NPQ conditions (Fig. 1, *A* and *B*). The NPQ state was induced by illuminating chloroplasts with high light for 30 min, and it was fixed by lowering the pH (from 7.6 to 5.0 units) of the chloroplast suspensions and keeping them at 4 °C (Fig. 1*C*). The quenching induction was performed on intact chloroplasts without using diaminodurene, to ensure that NPQ formation was comparable with that observed *in vivo*.

The sucrose density gradient profiles of the APol-trapped thylakoid membrane proteins showed mainly three pigmented bands, for both dark and NPQ conditions, which were assigned to the trimeric form of LHCII, PSI/LHCI/LHCII trimer, and the aggregated form of LHCII trimers (Fig. 1 and Figs. S3 and S4). Because the main focus of this work was to provide a methodology to isolate the aggregated LHCII that could occur in the thylakoid membrane, here we show the relative chlorophyll content of the bands associated to LHCII trimeric and aggregate states (Fig. 1). In violaxanthin-enriched samples, the ratio of trimer/aggregate relative chlorophyll content decreased ~2-fold from NPQ (~7:1) to dark state (~13:1) (Fig. 1*A*). These results demonstrate that LHCII complexes are partially aggregated in thylakoid membranes even under dark conditions and in the presence of violaxanthin, whereas LHCII aggregation increases upon the onset of NPQ.

Because previous reports suggested that zeaxanthin enhances LHCII aggregation *in vivo* and *in vitro* (25, 50–52), we tested our approach on zeaxanthin-enriched thylakoid membranes isolated from *NoM* plants depleted of photosystem core complexes. The obtained results showed that zeaxanthin-enriched dark thylakoid membranes have a reduced LHCII trimer/aggregate ratio of relative chlorophyll content (~6:1; Fig. 1*B*) compared with the same condition for violaxanthin-enriched membranes (Fig. 1*A*). Moreover, NPQ induction substantially increased the amount of LHCII aggregation observed (trimer/aggregate ratio ~2:1), in line with previous reports (26, 29). Both major sucrose density gradient bands of LHCII trimers and aggregates were found to comprise Lhcb1 protein (Fig. 1*D*).

Because previous reports revealed that isolated LHCII complexes could aggregate under low pH conditions (28), we tested whether the acidification of the chloroplast suspension used here to fix the NPQ state was responsible for the LHCII aggregation observed. This was assessed by using the cross-linker, dithiobis(succinimidyl propionate) (DSP), to fix the NPQ state of LHCII complexes, as previously reported (32). DSP, is a hydrophobic chemical reagent that easily diffuses through chloroplast membranes and acts quickly at low concentrations. The use of DSP to sustain NPQ has been already optimized and shown to be effective in *Spinacea oleracea* and *A. thaliana* chloroplasts (32). Here the NPQ state was fixed by adding 0.5 mM DSP, and the obtained thylakoid membranes were loaded onto sucrose density gradients (Fig. S5). In agreement with the results obtained by lowering the pH to fix NPQ (Fig. 1), the amount of LHCII aggregates found when DSP was employed was greater in the NPQ compared with the dark state (Fig. S5). This confirms that the modulation of LHCII aggregation observed in our procedure in response to high-light treatment was induced by NPQ formation, and fixing the NPQ state by lowering pH did not produce artifacts.

The isolated LHCII aggregates were highly pure

The purity of LHCII aggregate bands obtained was assessed using absorption spectroscopy, as well as SDS-PAGE (Fig. 2 and Figs. S3 and S4). Absorption spectra of LHCII aggregates were normalized to their respective maxima at the Q_y band. To correct the absorption spectrum of LHCII aggregates and take into account the contamination by PSI, PSI absorption spectra were subtracted from that of LHCII aggregates until absorption at 700 nm was approximately 0, as in isolated LHCII trimers (Fig. 2). Using this method, we calculated PSI contamination in LHCII aggregates, under all four conditions

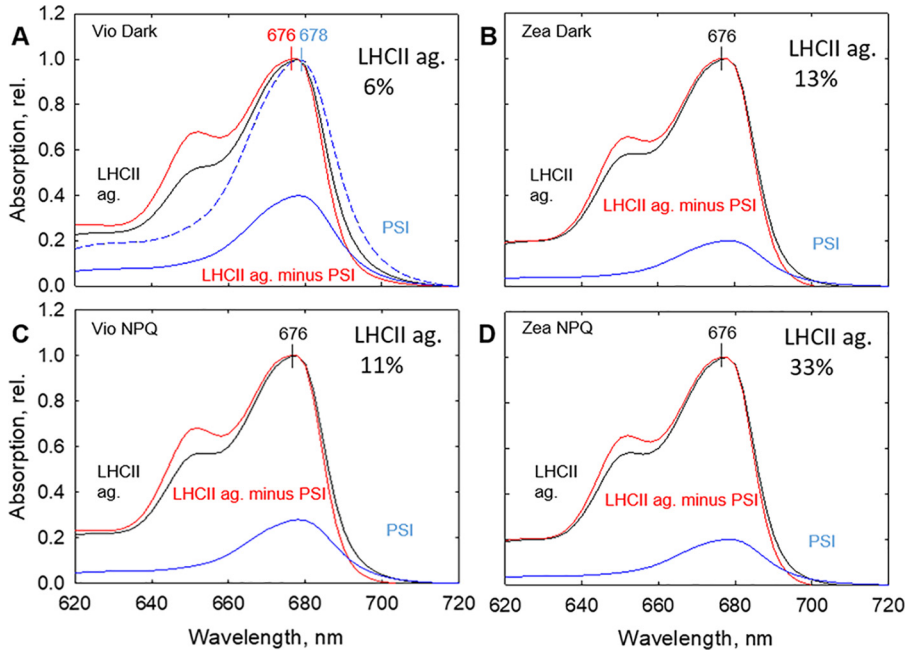

Figure 2. Absorption spectra of LHCII aggregates and assessment of PSI contamination. LHCII aggregates (*ag.*) enriched in violaxanthin (*A* and *C*) and zeaxanthin (*B* and *D*) are shown for dark-adapted and NPQ states. *Red lines* represent normalized absorption spectra of native LHCII aggregates corrected to remove PSI contamination (see Fig. 1 and S2). *Black lines* represent normalized absorption of uncorrected LHCII aggregates. *Dashed blue lines* represent the normalized absorption spectra of PSI. *Solid blue lines* represent the proportion of PSI subtracted from the uncorrected spectra to obtain the corrected LHCII aggregate spectra. In each panel, the corrected relative (*rel.*) contributions (%) of LHCII aggregates from Fig. 1 are indicated. *Viol*, violaxanthin; *Zea*, zeaxanthin.

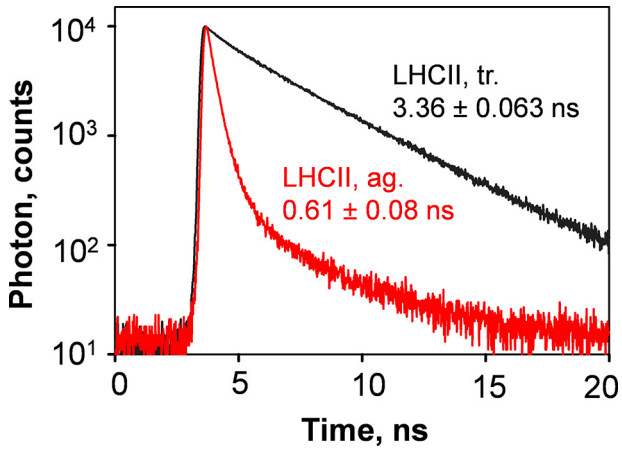

Figure 3. Fluorescence lifetime decay kinetics of isolated LHCII complexes. Shown are the time-correlated single-photon counting measurements of the sucrose density gradient bands of zeaxanthin-enriched LHCII trimers and aggregates, under NPQ conditions. Representative traces of LHCII trimers (*tr.*, *black trace*) and aggregates (*ag.*, *red trace*) are shown.

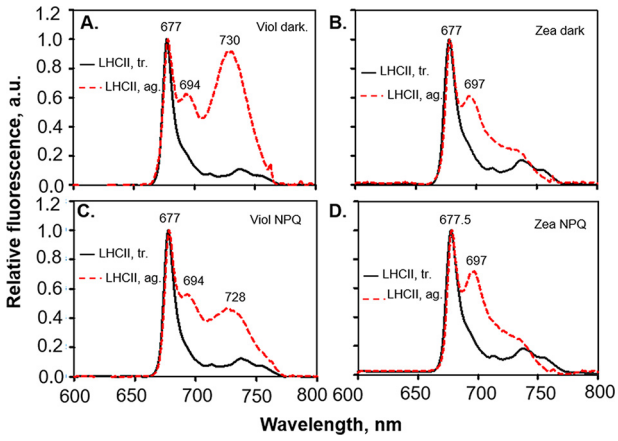

Figure 4. 77 K fluorescence emission spectra of LHCII trimers (*black lines*) and aggregates (*red dotted lines*). Violaxanthin-enriched (*A* and *C*) and zeaxanthin-enriched thylakoid membranes (*B* and *D*), in dark-adapted and NPQ states are shown. Emission spectra were recorded from sucrose density gradient bands of the solubilized thylakoid membranes (see Fig. 1). Representative emission spectra are shown for each condition. *ag.*, aggregate; *a.u.*, arbitrary unit(s); *tr.*, trimers; *Viol*, violaxanthin; *Zea*, zeaxanthin.

tested (violaxanthin- and zeaxanthin-enriched membranes, dark and NPQ conditions; Fig. 1). Fig. 2 reveals that the contamination of PSI in LHCII aggregate bands was negligible (ranging from 1 to 3%). The purity of the sucrose density bands was also assessed by SDS-PAGE and Western blotting analyses (Figs. S3 and S4), which were in line with absorption data. Moreover, SDS-PAGE results showed almost complete absence of RCIIs, as well as very little PSI contamination in the aggregated LHCII bands. The low contamination of PSI in the aggregated bands was also confirmed by Western blotting (Figs. S3 and S4).

The isolated, native LHCII aggregates were strongly quenched

Fluorescence lifetime decay kinetics were measured on LHCII trimers and aggregates isolated from sucrose density gradients to compare the degree of chlorophyll fluorescence quenching in these pigment–protein complexes. Fig. 3 shows representative time-resolved fluorescence lifetime decay kinetics of LHCII trimers and LHCII aggregates isolated from zeaxanthin-enriched *NoM* thylakoid membrane in the NPQ state. The intensity-weighted lifetimes of LHCII trimers obtained in the four conditions tested (*i.e.* dark and NPQ states, for violaxanthin- and

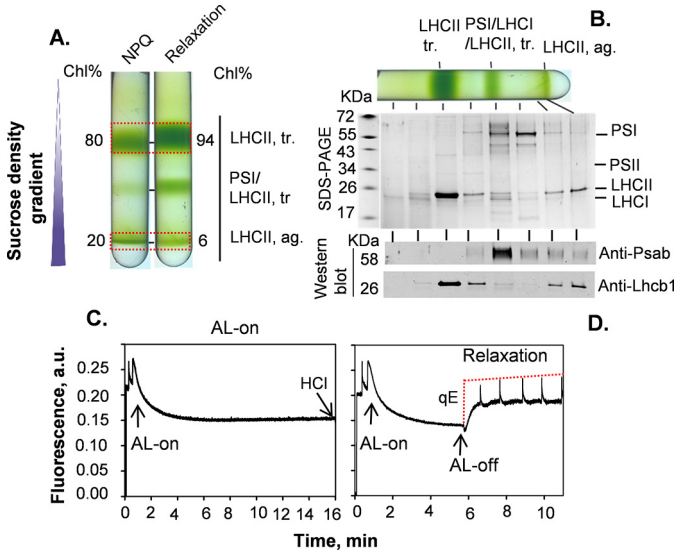

Figure 5. Purification and characterization of sucrose density-harvested LHCII bands under NPQ and relaxation states. *A*, isolation of the LHCII trimers (*tr.*) and aggregates (*ag.*) from solubilized photosynthetic membranes obtained from protoplasts, by sucrose density gradient. Violaxanthin-enriched *NoM* plants devoid of photosystem cores, under NPQ and relaxation states, were used. *B*, SDS-PAGE of samples fractionated by sucrose density gradients, after relaxation in the dark (*relaxation* in *A*). Western blotting analysis of PSI (PsaB) and Lhcb1 proteins is shown. *C* and *D*, representative PAM fluorescence quenching traces of *NoM* chloroplasts, obtained from protoplasts, used to induce NPQ (*C*) and recovery state (*D*), respectively. NPQ was fixed by lowering the pH from 7.6 to 5.0 adding 2 M HCl. *AL-off*, actinic light off; *AL-on*, actinic light on; *a.u.*, arbitrary unit(s); *Chl*, chlorophyll.

zeaxanthin-enriched membranes) were similar and ranged from ~3.3 to 3.5 ns (data not shown). These values were consistent with those measured on detergent-solubilized LHCII trimers and LHCII trimers trapped in nanodiscs (19, 53). In agreement with average lifetimes reported for the artificially induced LHCII aggregates by detergent removal (54, 55), the average (intensity-weighted) lifetimes of the APol-trapped LHCII aggregates were ~0.6 ns and substantially lower than those of isolated LHCII trimers (Fig. 3 and Table S1). This indicates that the LHCII aggregates isolated were strongly quenched. Although for zeaxanthin-enriched LHCII trimers isolated in NPQ state the intensity-weighted lifetime component of ~3.8 ns showed the greatest contribution (~75%), LHCII aggregates displayed a substantial shortening of the lifetime components (Table S1).

Low-temperature (77 K) fluorescence emission spectra of LHCII trimers and LHCII aggregates were measured (Fig. 4). The emission spectrum of LHCII trimers isolated under the four conditions tested showed a peak ~680 nm (51, 56). Notably, the emission spectra of the APol-trapped LHCII aggregates showed a second peak near 698 nm (Fig. 4). This red-shifted peak is remarkably similar to the emission measured on LHCII oligomers, induced *in vitro*, after detergent removal (51, 57–59). In addition, the spectrum of our isolated aggregates resembles that of the thylakoid membranes devoid of PSII core and depleted from PSI complexes (33). The second red-shifted fluorescence peak could not originate from PSII cores because our thylakoid membranes were also lacking PSII cores (Figs. S2 and S3).

The aggregated LHCIIs obtained from sucrose density gradient of violaxanthin-enriched thylakoid membranes showed an emission peak centered at ~730 nm (Fig. 4, *A* and *C*). For zeaxanthin-enriched LHCII aggregates, a less-pronounced shoulder appeared in the same region (~730 nm; Fig. 4, *B* and *D*). Such long-wavelength emission band originates from PSI, and its lower contribution in zeaxanthin-enriched LHCII aggregates relative to violaxanthin-enriched ones is due to a reduced contamination of PSI cores in the former samples (Fig. 2 and Figs. S3 and S4).

The NPQ-induced aggregation of LHCII proteins is reversible

The chloroplast preparations from lincomycin-treated *Arabidopsis NoM* plants depleted of RCIIs used in this work were able to form NPQ, however, showing little recovery in the dark. To probe whether the native LHCII aggregates here isolated were also able to recover from quenching in the dark, we prepared chloroplasts from protoplasts (Fig. 5), using a more gentle procedure previously used (24, 60). Chloroplasts obtained by this methodology were capable of forming qE more quickly (Fig. 5*C*) than those prepared using a less gentle procedure (Fig. 1*C*), and, most importantly, reversible in the dark (Fig. 5*D*). Photosynthetic membranes isolated from protoplast preparations were solubilized using the same conditions used for chloroplast preparations (Fig. 1), and both the NPQ and recovery states were investigated (Fig. 5, *C* and *D*).

The obtained sucrose density gradient profiles (Fig. 5*A*) were similar to those observed for chloroplast preparations (Fig. 1*A*). The purity of the sucrose density bands was judged by SDS-PAGE, showing the presence of single protein bands at ~25 kDa, identified by Western blotting as Lhcb1 protein (Fig. 5*B*). Fig. 5*B* revealed that LHCII polypeptides (*e.g.* Lhcb1) were the main protein components of all pigmented bands isolated, indicating that the different aggregation states corresponded to LHCIIs. At the same time, LHCII trimers appeared to co-migrate with PSI core proteins, with a minor contribution of PSI for LHCII aggregates (Fig. 5*B*). Nonetheless, the purity of the LHCII aggregate bands was high, with 1–4% of PSI contamination in both conditions (Fig. 6).

Discussion

Over the past few decades, the LHCII aggregation model has gradually been accepted as the process underlying qE (25, 26, 61). The aggregated LHCII induces conformational changes within the LHCII antenna complexes that ultimately form the quencher (8, 26). As a result, the fluorescence lifetime of the aggregated LHCII is shorter than that of isolated LHCII (19, 50). Four different structural/functional states of LHCII antenna were identified, controlled by violaxanthin de-epoxidation, as well as protonation of LHCII antenna complexes (26). Briefly, the aggregation model suggests that LHCII is present in the unquenched state in the dark with violaxanthin presence (state I). Upon illumination, de-epoxidation of violaxanthin and protonation of LHCII drives the system into the quenched state by promoting LHCII aggregation (state IV). If zeaxanthin is not formed, LHCII will be only partially quenched (state III). If zeaxanthin is present, LHCII antenna remains partially aggregated and therefore quenched (state II). The aim of

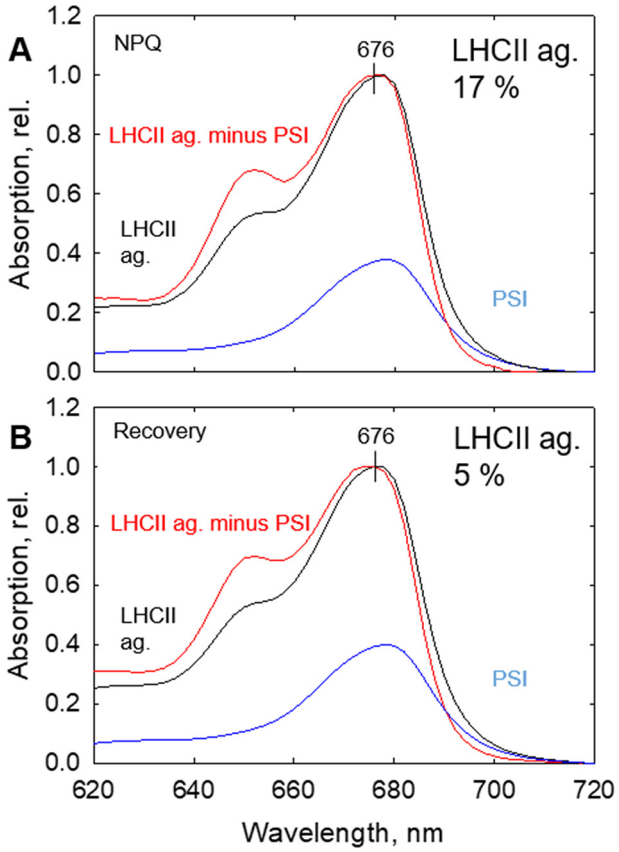

Figure 6. Absorption spectra of LHCII aggregates obtained from protoplast preparations. PSI contamination was estimated for NPQ (*A*) and recovery states (*B*). *Red lines* represent normalized absorption spectra of natural LHCII aggregates (*ag.*) corrected to remove PSI contamination (see Fig. 5). *Black lines* represent normalized absorption of the uncorrected LHCII aggregates. *Solid blue lines* represent the proportion of PSI subtracted from the uncorrected spectra to obtain the corrected LHCII aggregate spectra. *rel.*, relative.

this work was to isolate and characterize the LHCII in these structural/functional states from photosynthetic membranes.

LHCII aggregation and consequent NPQ formation have been investigated and demonstrated *in vitro* by using detergent removal to induce aggregation of isolated LHCII trimers (51, 54, 61, 62). Spectroscopic studies either performed *in vivo* (intact leaves) (63) or *in vitro* (50, 64) provided convincing data suggesting that the quenched conformation of LHCII is controlled by xanthophyll cycle activity that influences the aggregation state of LHCII proteins (4, 50, 65). Furthermore, it has been shown that the amount of LHCII aggregation correlates with the amount of NPQ (26). Moreover, direct evidence that LHCII antenna undergoes reorganization within the thylakoid membrane in response to light treatment and darkness, as well as ΔpH and zeaxanthin synthesis, was obtained by freeze fracture EM data on intact spinach chloroplasts (29). These studies suggest that zeaxanthin acts as an allosteric regulator of NPQ, which promotes this process by inducing the aggregated state of LHCII. Another allosteric factor that influences the oligomeric state of LHCII and consequent qE formation is PsbS. However, zeaxanthin and PsbS works differently in relation to qE, especially in the relaxation phase. Although zeaxanthin slows qE relaxation, PsbS promotes both quick qE formation as well as relaxation. In addition, increased levels of PsbS enhance qE, in both the presence and the absence of zeaxanthin. This suggests that zeaxanthin and PsbS have different roles in qE formation, and thus the direct role of these allosteric factors should be investigated separately.

Detergents have been routinely used to efficiently solubilize, isolate, and study the function of photosynthetic membrane protein complexes, such as the major trimeric LHCII antenna. However, detergents are also known to cause loss of weak interactions, such as those between LHCII trimers. Furthermore, detergents can cause the production of free LHCII trimers, which does not reflect the native state of LHCII within the photosynthetic membranes. This has been a long-standing issue when it comes to the isolation of native LHCII in the aggregated, quenched form. In this work, we used a combination of mild detergent (digitonin and α-DM) and APols to efficiently isolate and stabilize LHCII complexes in different native states (*i.e.* trimers and large aggregates) (40, 41, 44), aiming to isolate the LHCII aggregates within the thylakoid membrane during NPQ formation and thereby validating the aggregation model. The main advantage of using these polymers over detergents alone is being able to isolate large protein complexes in their close-to-native form. Previously, APols have been used to investigate structural and functional aspects of membrane proteins, including photosynthetic complexes (44–46, 66). APols bind noncovalently to the hydrophobic surface of the membrane proteins with an extremely slow dissociation rate (40). This makes their association with membrane proteins more stable (67–69), even at extreme dilution (69). Upon being trapped with APols, detergent-solubilized membrane proteins remain in the native conformational organization that they were in before detergent removal (40, 44, 45, 70). Therefore, the use of APols rules out the possibility of artificially induced aggregation of the membrane proteins. Thus, using these polymers provides an opportunity to investigate the aggregation state of LHCII complexes free of artifacts. APol-trapped LHCII complexes are therefore likely to reflect their native state, thus providing biochemical evidence for the presence of the four structural/functional states proposed in (25).

Here, we show the direct experimental evidence that LHCII antenna aggregation is controlled by the xanthophyll cycle activity and the degree of quenching occurring *in vivo*. Our results demonstrate the direct involvement of xanthophylls in controlling the different aggregated states of the LHCII antenna, with zeaxanthin promoting the aggregation process (Fig. 1) (25, 26). We observed that LHCII complexes containing violaxanthin can still form aggregates even in the dark (Fig. 1*A*). However, the amount of LHCII aggregates was lower compared with those obtained in zeaxanthin-enriched LHCIIs in the dark. In the NPQ state, the amount of aggregated LHCIIs was further enhanced compared with those obtained in the dark (Fig. 1). These data directly relate NPQ formation with the aggregation of LHCII complexes. Here, it should be noted that the amount of the aggregated LHCII was enhanced by NPQ induction that further increases upon zeaxanthin accumulation. Regardless of the type of xanthophyll present (either violaxanthin or zeaxanthin), the fluorescence lifetime of the aggregated LHCIIs was highly reduced relative to that of free LHCII

trimers. This supports previous data suggesting that NPQ possesses similar features, regardless of the presence of either violaxanthin or zeaxanthin (71, 72). Both the highly reduced chlorophyll fluorescence lifetime of the aggregated LHCIIs and isolation of the aggregated LHCIIs from either dark or violaxanthin-enriched thylakoid membranes support the notion that in the thylakoid membrane, LHCII complexes are always present in partially aggregated/quenched form (19). Upon illumination with high light, LHCII antenna aggregation further increases.

Our data support the view that zeaxanthin enhances quenching by causing conformational changes in LHCII antenna complexes, facilitating their transition into the aggregated state. The hydrophobic properties of the xanthophyll pigments have been proposed to influence LHCII aggregation (50). Being the most hydrophobic xanthophyll, zeaxanthin favors the formation of LHCII aggregates, thereby enhancing quenching, whereas the more polar violaxanthin promotes the unaggregated state of LHCII (9, 28, 50). In this regard, 77 K fluorescence emission measurements of the aggregated LHCII (Fig. 4) support the appearance of a broad long-wavelength band at 700 nm, which appears upon aggregation of LHCII trimers (73). This band has been used as a fingerprint of LHCII aggregation (57, 58, 73). Interestingly, this red-shifted fluorescence was prominent in the LHCII crystal that produced higher levels of structural homogeneity and displayed a fluorescence lifetime consistent with LHCII complexes in the quenched state (51, 74).

In conclusion, this study provides direct, experimental evidence of the LHCII aggregation model for qE regulation (26). Using a novel purification methodology, we show that the formation of qE naturally occurring within the thylakoid membrane is controlled by the activity of the xanthophyll pigments. This results in the presence of different native organizations of LHCII antenna. Although zeaxanthin promotes the quenched state by enhancing the amount of LHCII clusters, violaxanthin inhibits LHCII aggregation and quenching. The different effect of xanthophyll pigments on LHCII aggregation could reflect the distinct hydrophobic properties of these pigments (9). This novel method allows for the isolation of LHCII antenna complexes, in highly pure and close-to-native states, from the thylakoid membranes. The isolation of these native LHCII aggregates is instrumental to further study pigment–protein interactions within LHCII complexes, as well as energy transfer pathways under light-harvesting and NPQ conditions.

Experimental procedures

Plant growth conditions

A. thaliana NoM (No Minor antennae mutant) (19) plants were used in this study. The seeds were sterilized in 50% ethanol and 0.1% Triton X-100 and stored for 72 h at 4 °C prior to sowing (23). The plants were grown on a 6:6:1 ratio of John Innes No. 3 soil, Levington M3 potting compost and perlite (Scotts UK, Ipswich, UK). The seedlings were grown under 180 μmol photons m^{-2} s^{-1} in a 10-h day/14-h night photoperiod at 22 °C. The plants were treated with lincomycin (0.4–0.8 g $liter^{-1}$) at the full rosette growth stage for a period of 2–3 weeks, until the F_v/F_m value of the leaves was reduced to 0.2 or less. The plants were able to survive lincomycin treatments for several weeks, although at a reduced growth rate compared with WT plants. The leaves were enriched in zeaxanthin by illumination with white light (550 μmol photons m^{-2} s^{-1}) and under 98% N_2:2% O_2, for 2 h before chloroplast or protoplast isolation. To ensure complete violaxanthin de-epoxidation, the chloroplasts were further incubated in de-epoxidation buffer (0.33 M sorbitol, 1 mM EDTA, 30 mM HEPES, 20 mM MES, 40 mM ascorbate, pH 5.5) in the dark for 30 min (49).

Preparation of protoplasts, chloroplasts, and thylakoid membranes

Mesophyll cell protoplasts were prepared by enzymatic digestion of cell walls of leaves (60). Briefly, the lower epidermis of the leaves was stripped with adhesive tape followed by incubation on a buffer solution (0.4 M mannitol, 20 mM KCl, 20 mM MES, 10 mM $CaCl_2$, 0.1% BSA, pH 5.5) containing 1.5% Cellulose Onuzuka R-10 and 0.4% macerozyme R-10 (Serva) for 1 h. The released protoplasts in the solution were filtered in one layer of muslin cloth and centrifuged twice at 100 relative centrifugation field (RCF) at 4 °C. The pelleted protoplasts were then resuspended in reaction buffer containing 0.5 M sorbitol, 20 mM HEPES, 20 mM MES, 20 mM sodium citrate, 10 mM EDTA, 10 mM $NaHCO_3$, 15 mM $MgCl_2$, 0.1% BSA (pH 7.6). Chloroplasts were prepared by osmotic shock of the protoplasts (24). Intact chloroplasts were also prepared by direct homogenization of the leaves in ice-cold grinding solution (330 mM sorbitol, 5 mM $MgCl_2$, 10 mM $Na_4P_2O_7$, 2.5 mM EDTA, pH 6.5, 40 mM D-isoascorbate) according to Townsend *et al.* (23). The homogenized solution was filtered through four layers of muslin cloth, then four layers of muslin cloth with a layer of nonadhesive cotton wool, and finally resuspended in the resuspension buffer (0.3 M sorbitol, 2.5 mM EDTA, 5 mM $MgCl_2$, 10 mM $NaHCO_3$, 20 mM HEPES, 0.5% (w/v) BSA, pH 7.6). Thylakoid membranes were prepared by incubating the chloroplast in breaking buffer (5 mM NaCl, 5 mM $MgCl_2$, 10 mM HEPES, pH 7.5) for 30 s, followed by centrifugation at 14,000 rpm for 1.5 min at 4 °C. The obtained thylakoid membranes were suspended in buffer B (330 mM sorbitol, 5 mM $MgCl_2$, 10 mM KCl, 2.5 mM EDTA, 20 mM HEPES, pH 7.6).

Chlorophyll fluorescence induction

Chlorophyll fluorescence of violaxanthin- and zeaxanthin-enriched chloroplasts was measured with a Dual-PAM-100 fluorometer (Walz). The fluorescence level with PSII reaction centers open (F_o) was measured with a 2 μmol photons m^{-2} s^{-1} measuring light. The maximum fluorescence values in the dark-adapted state (F_m) and during actinic illumination (F_m') were measured using a 0.8-s saturating light pulse (4,000 μmol photons m^{-2} s^{-1}). Fluorescence quenching was induced in chloroplast suspensions by using an actinic light intensity of 1,380 μmol photons m^{-2} s^{-1} for 30 min. For chloroplasts prepared from protoplasts, fluorescence quenching was induced by actinic light at lower intensity (488 μmol photons m^{-2} s^{-1}) for 16 min. Far red (20 μmol photons m^{-2} s^{-1}) light was used in the dark to preferentially excite PSI and reoxidize the

plastoquinone pool and PSII during fluorescence recovery. Samples were collected in the dark, NPQ, and recovery states for further analysis. The NPQ state was sustained by reducing the pH of the chloroplast suspension from pH 7.6 to pH 5.0 at 4 °C (32).

Purification of aggregated LHCII complexes

Seven-step exponential sucrose density gradients were prepared as previously described (36). A 20 mM HEPES (pH 7.8) buffer was employed in the preparation of sucrose solutions. The solubilized thylakoid membranes were prepared as described by Watanabe *et al.* (44) with slight modifications. Thylakoid membranes (total chlorophyll concentration corresponding to 0.5 mg ml^{-1}), in the dark, NPQ, and recovery states were treated with 0.3% α-DM + 0.5% digitonin for 30 min on ice. To load an equal amount of total chlorophyll in each tube (*i.e.* 500 μl of 0.5 mg chlorophyll ml^{-1}), we prepared thylakoid membranes solubilized with detergents (α-DM and digitonin) in excess volume (600 μl). The unsolubilized material was removed by centrifugation at 14,000 rpm for 5 min at 4 °C. Subsequently, APol A8–35 (Anatrace) was added to the solubilized thylakoid membranes at a final concentration of 1% (w/v) to stabilize the protein complexes therein, followed by 10 min dark incubation on ice. The APol-stabilized pigment–protein complexes were loaded (final concentration was 0.25 mg chlorophyll/tube) onto sucrose density gradient tubes, and protein complexes were fractionated by ultracentrifugation using a swinging bucket rotor (SW41 Ti, Beckman Coulter, UK) for 17 h, at 40,000 rpm and at 4 °C (Optima L-80 XP ultracentrifuge; Beckman Coulter). For these experiments, no detergent was added in the sucrose solutions to facilitate removal of the remaining detergent in the course of centrifugation and thus to allow all the pigment–protein complexes to be efficiently and solely trapped by APols. Sucrose gradient bands were collected and kept on ice until further measurements.

Absorption spectroscopy

Absorption measurements were carried out using an Aminco DW-2000 UV/Vis spectrophotometer (Olis Inc.). The absorption spectra were recorded between 350 and 750 nm in 1-nm increments. The relative chlorophyll content of LHCII trimer and aggregate bands was determined by integrating the area from 600 to 750 nm below each spectrum as $[\mathrm{Chl}] = (\int_{600}^{750} A(\lambda) \times d(\lambda) \times V \times D$, where $\int_{600}^{750} A(\lambda) \times d(\lambda)$ is the integral of the absorption in function of wavelength, V is the volume of the sucrose density band, and D is the dilution factor applied to sample prior to the acquisition of absorption spectrum. To correct the LHCII aggregate band spectrum to account for the contamination by PSI observed, absorption spectra were normalized to their respective maxima at the Q_y band, and the PSI spectra were subtracted from the aggregate spectra until the resulting spectrum matched that of an LHCII trimer. To then work out the percentage of PSI contamination in the LHCII aggregate band, the areas under the spectra between 676 and 720 nm were calculated. The decrease in area between the raw and corrected LHCII aggregate band spectra was determined to be the percentage of PSI contamination.

Low-temperature steady-state fluorescence spectroscopy

Low-temperature (77 K) emission spectra were measured with FluoroMax-3 spectrophotometer (HORIBA Jobin Yvon, Longjumeau, France) equipped with a cryostat cooled by liquid nitrogen. The samples were excited at 435 nm, and emission was acquired from 600 to 800 nm, at 1.0-nm emission spectral resolution. Five scans were taken for each spectrum and then averaged. Fluorescence excitation spectra were corrected for variations in the detector efficiency and excitation lamp intensity and distribution with files provided by the manufacturer.

Chlorophyll fluorescence lifetime measurement

Time-correlated single-photon counting measurements were performed using a FluoTime 200-ps fluorometer (PicoQuant, Berlin, Germany) (62). Briefly, fluorescence lifetime decay kinetics were measured on sucrose density bands of LHCII (trimers and aggregates). Excitation was provided at a 20-MHz repetition rate by a 468-nm laser diode. The fluorescence was detected at 682 nm with a 1-nm slit width. The instrument response function was ~50 ps. FluoFit software (PicoQuant, Germany) was used to analyze fluorescence lifetime data by a multiexponential model with iterative reconvolution of the instrument response function. The fluorescence lifetime data were analyzed using FluoFit software (PicoQuant), and the quality of the fit was determined by the χ^2 parameter.

SDS-PAGE and Western blotting

Protein complexes of each sucrose density gradient bands were separated by SDS-PAGE, using 16% Tricine–SDS–PAGE gels (46). Equal volumes (20 μl) of pigmented bands collected from sucrose density gradients were loaded into each lane. The gels were stained using InstantBlue protein stain (Expedeon) and scanned using a ChemiDoc touch imaging system (Bio-Rad). Proteins separated by SDS-PAGE were transferred onto cellulose membrane (GE Healthcare) and identified by Western blotting. Anti-Lhcb1 (1:2,000, AS01004; Agrisera) and PsaB (1:1,000, AS10695; Agrisera) antibodies were used. Antibody signals were detected after incubation with a secondary goat anti-rabbit antibody (IRDye 800CW; LI-COR Biosciences Ltd.; 1:20,000) and visualized by near IR fluorescence detection (Odyssey imaging system; LI-COR Biosciences Ltd.).

Data availability

All the data are located in the Ruban laboratory data storage facility (http://research.sbcs.qmul.ac.uk/a.ruban/) and can be made available upon request sent to a.ruban@qmul.ac.uk.

Author contributions—M. K. S., A. W., V. G., E. I. M., and A. V. R. data curation; M. K. S., A. W., and E. I. M. formal analysis; M. K. S. and A. V. R. validation; M. K. S., S. W., V. G., E. I. M., and A. V. R. investigation; M. K. S., A. W., S. W., E. I. M., J. M., and A. V. R. methodology; M. K. S. writing-original draft; V. G., J. M., and A. V. R. writing-review and editing; J. M. and A. V. R. supervision;

A. V. R. conceptualization; A. V. R. funding acquisition; A. V. R. project administration.

Funding and additional information—This work was supported by Biotechnology and Biological Sciences Research Council Grant BB/R015694/1, Leverhulme Trust Grant RPG-2018-199, and Royal Society International Exchanges Standard Scheme Grant IES\R2\170087 (to A. V. R.). The collaboration between the Ruban and Minagawa laboratories was supported by Royal Society Grant IES\R2\170087.

Conflict of interest—The authors declare that they have no conflicts of interest with the contents of this article.

Abbreviations—The abbreviations used are: NPQ, nonphotochemical quenching; LHC, light-harvesting complex; PS, photosystem; RC, reaction center; qE, energy-dependent quenching; APol, amphipol; DSP, dithiobis(succinimidyl propionate); α-DM, n-dodecyl-α-D-maltoside.

References

1. Blankenship, R. E. (2014) *Molecular Mechanisms of Photosynthesis*, John Wiley & Sons, New York
2. Jansson, S. (1999) A guide to the Lhc genes and their relatives in *Arabidopsis*. *Trends Plant Sci.* **4,** 236–240 CrossRef Medline
3. Barber, J. (1995) Molecular basis of the vulnerability of photosystem II to damage by light. *Funct. Plant Biol.* **22,** 201–208 CrossRef
4. Demmig-Adams, B., and Adams, W. W., 3rd (1992) Photoprotection and other responses of plants to high light stress. *Annu. Rev. Plant Biol.* **43,** 599–626 CrossRef
5. Powles, S. B. (1984) Photoinhibition of photosynthesis induced by visible light. *Annu. Rev. Plant Physiol.* **35,** 15–44 CrossRef
6. Li, Z., Wakao, S., Fischer, B. B., and Niyogi, K. K. (2009) Sensing and responding to excess light. *Annu. Rev. Plant Biol.* **60,** 239–260 CrossRef Medline
7. Ruban, A. V. (2016) Nonphotochemical chlorophyll fluorescence quenching: mechanism and effectiveness in protecting plants from photodamage. *Plant Physiol.* **170,** 1903–1916 CrossRef Medline
8. Ruban, A. V. (2018) Light harvesting control in plants. *FEBS Lett.* **592,** 3030–3039 CrossRef Medline
9. Ruban, A. V., Johnson, M. P., and Duffy, C. D. (2012) The photoprotective molecular switch in the photosystem II antenna. *Biochim. Biophys. Acta* **1817,** 167–181 CrossRef Medline
10. Li, X. P., Björkman, O., Shih, C., Grossman, A. R., Rosenquist, M., Jansson, S., and Niyogi, K. K. (2000) A pigment-binding protein essential for regulation of photosynthetic light harvesting. *Nature* **403,** 391–395 CrossRef Medline
11. Li, X.-P., Gilmore, A. M., Caffarri, S., Bassi, R., Golan, T., Kramer, D., and Niyogi, K. K. (2004) Regulation of photosynthetic light harvesting involves intrathylakoid lumen pH sensing by the PsbS protein. *J. Biol. Chem.* **279,** 22866–22874 CrossRef Medline
12. Correa-Galvis, V., Poschmann, G., Melzer, M., Stühler, K., and Jahns, P. (2016) PsbS interactions involved in the activation of energy dissipation in *Arabidopsis*. *Nat. Plants* **2,** 15225 CrossRef Medline
13. Kromdijk, J., Głowacka, K., Leonelli, L., Gabilly, S. T., Iwai, M., Niyogi, K. K., and Long, S. P. (2016) Improving photosynthesis and crop productivity by accelerating recovery from photoprotection. *Science* **354,** 857–861 CrossRef Medline
14. Krieger, A., Moya, I., and Weis, E. (1992) Energy-dependent quenching of chlorophyll a fluorescence: effect of pH on stationary fluorescence and picosecond-relaxation kinetics in thylakoid membranes and photosystem II preparations. *Biochim. Biophys. Acta* **1102,** 167–176 CrossRef
15. Horton, P., and Ruban, A. (1992) Regulation of photosystem II. *Photosynth. Res.* **34,** 375–385 CrossRef Medline
16. Ahn, T. K., Avenson, T. J., Ballottari, M., Cheng, Y.-C., Niyogi, K. K., Bassi, R., and Fleming, G. R. (2008) Architecture of a charge-transfer state regulating light harvesting in a plant antenna protein. *Science* **320,** 794–797 CrossRef Medline
17. Ruban, A. V., Berera, R., Ilioaia, C., Van Stokkum, I. H., Kennis, J. T., Pascal, A. A., Van Amerongen, H., Robert, B., Horton, P., and Van Grondelle, R. (2007) Identification of a mechanism of photoprotective energy dissipation in higher plants. *Nature* **450,** 575–578 CrossRef Medline
18. Bergantino, E., Segalla, A., Brunetta, A., Teardo, E., Rigoni, F., Giacometti, G. M., and Szabò, I. (2003) Light- and pH-dependent structural changes in the PsbS subunit of photosystem II. *Proc. Natl. Acad. Sci. U.S.A.* **100,** 15265–15270 CrossRef Medline
19. Belgio, E., Johnson, M. P., Jurić, S., and Ruban, A. V. (2012) Higher plant photosystem II light-harvesting antenna, not the reaction center, determines the excited-state lifetime: both the maximum and the nonphotochemically quenched. *Biophys. J.* **102,** 2761–2771 CrossRef Medline
20. Dominici, P., Caffarri, S., Armenante, F., Ceoldo, S., Crimi, M., and Bassi, R. (2002) Biochemical properties of the PsbS subunit of photosystem II either purified from chloroplast or recombinant. *J. Biol. Chem.* **277,** 22750–22758 CrossRef Medline
21. Johnson, M. P., and Ruban, A. V. (2011) Restoration of rapidly reversible photoprotective energy dissipation in the absence of PsbS protein by enhanced ΔpH. *J. Biol. Chem.* **286,** 19973–19981 CrossRef Medline
22. Dall'Osto, L., Cazzaniga, S., Bressan, M., Paleček, D., Žídek, K., Niyogi, K. K., Fleming, G. R., Zigmantas, D., and Bassi, R. (2017) Two mechanisms for dissipation of excess light in monomeric and trimeric light-harvesting complexes. *Nat. Plants* **3,** 17033 CrossRef Medline
23. Townsend, A. J., Saccon, F., Giovagnetti, V., Wilson, S., Ungerer, P., and Ruban, A. V. (2018) The causes of altered chlorophyll fluorescence quenching induction in the *Arabidopsis* mutant lacking all minor antenna complexes. *Biochim. Biophys. Acta* **1859,** 666–675 CrossRef Medline
24. Saccon, F., Giovagnetti, V., Shukla, M. K., and Ruban, A. V. (2020) Rapid regulation of photosynthetic light harvesting in the absence of minor antenna and reaction centre complexes. *J. Exp. Bot.* **71,** 3626–3637 CrossRef Medline
25. Horton, P., Ruban, A., Rees, D., Pascal, A., Noctor, G., and Young, A. (1991) Control of the light-harvesting function of chloroplast membranes by aggregation of the LHCII chlorophyll–protein complex. *FEBS Lett.* **292,** 1–4 CrossRef Medline
26. Horton, P., Wentworth, M., and Ruban, A. (2005) Control of the light harvesting function of chloroplast membranes: the LHCII-aggregation model for non-photochemical quenching. *FEBS Lett.* **579,** 4201–4206 CrossRef Medline
27. Horton, P., Ruban, A. V., and Wentworth, M. (2000) Allosteric regulation of the light-harvesting system of photosystem II. *Philos. Trans. R. Soc. Lond. B Biol. Sci.* **355,** 1361–1370 CrossRef Medline
28. Ruban, A. V., Young, A., and Horton, P. (1994) Modulation of chlorophyll fluorescence quenching in isolated light harvesting complex of photosystem II. *Biochim. Biophys. Acta* **1186,** 123–127 CrossRef
29. Johnson, M. P., Goral, T. K., Duffy, C. D. P., Brain, A. P. R., Mullineaux, C. W., and Ruban, A. V. (2011) Photoprotective energy dissipation involves the reorganization of photosystem II light-harvesting complexes in the grana membranes of spinach chloroplasts. *Plant Cell* **23,** 1468–1479 CrossRef Medline
30. Betterle, N., Ballottari, M., Zorzan, S., de Bianchi, S., Cazzaniga, S., Dall'Osto, L., Morosinotto, T., and Bassi, R. (2009) Light-induced dissociation of an antenna hetero-oligomer is needed for non-photochemical quenching induction. *J. Biol. Chem.* **284,** 15255–15266 CrossRef Medline
31. Horton, P., Ruban, A., and Walters, R. (1996) Regulation of light harvesting in green plants. *Annu. Rev. Plant Biol.* **47,** 655–684 CrossRef Medline
32. Sacharz, J., Giovagnetti, V., Ungerer, P., Mastroianni, G., and Ruban, A. V. (2017) The xanthophyll cycle affects reversible interactions between PsbS and light-harvesting complex II to control non-photochemical quenching. *Nat. Plants* **3,** 16225 CrossRef Medline
33. Goral, T. K., Johnson, M. P., Duffy, C. D., Brain, A. P., Ruban, A. V., and Mullineaux, C. W. (2012) Light-harvesting antenna composition controls

the macrostructure and dynamics of thylakoid membranes in *Arabidopsis*. *Plant J.* **69,** 289–301 CrossRef Medline
34. Ware, M. A., Giovagnetti, V., Belgio, E., and Ruban, A. V. (2015) PsbS protein modulates non-photochemical chlorophyll fluorescence quenching in membranes depleted of photosystems. *J. Photoch. Photobiol. B* **152,** 301–307 CrossRef Medline
35. Noctor, G., Ruban, A. V., and Horton, P. (1993) Modulation of ΔpH-dependent nonphotochemical quenching of chlorophyll fluorescence in spinach chloroplasts. *Biochim. Biophys. Acta* **1183,** 339–344 CrossRef
36. Ruban, A. V., Lee, P. J., Wentworth, M., Young, A. J., and Horton, P. (1999) Determination of the stoichiometry and strength of binding of xanthophylls to the photosystem II light harvesting complexes. *J. Biol. Chem.* **274,** 10458–10465 CrossRef Medline
37. Eijckelhoff, C., Dekker, J. P., and Boekema, E. J. (1997) Characterization by electron microscopy of dimeric photosystem II core complexes from spinach with and without CP43. *Biochim. Biophys. Acta* **1321,** 10–20 CrossRef
38. Boekema, E. J., van Roon, H., Calkoen, F., Bassi, R., and Dekker, J. P. (1999) Multiple types of association of photosystem II and its light-harvesting antenna in partially solubilized photosystem II membranes. *Biochemistry* **38,** 2233–2239 CrossRef Medline
39. Tribet, C., Audebert, R., and Popot, J.-L. (1996) Amphipols: polymers that keep membrane proteins soluble in aqueous solutions. *Proc. Natl. Acad. Sci. U.S.A.* **93,** 15047–15050 CrossRef Medline
40. Popot, J.-L., Althoff, T., Bagnard, D., Banères, J.-L., Bazzacco, P., Billon-Denis, E., Catoire, L. J., Champeil, P., Charvolin, D., Cocco, M. J., Crémel, G., Dahmane, T., de la Maza, L. M., Ebel, C., Gabel, F., *et al.* (2011) Amphipols from A to Z. *Annu. Rev. Biophys.* **40,** 379–408 CrossRef Medline
41. Zoonens, M., Catoire, L. J., Giusti, F., and Popot, J.-L. (2005) NMR study of a membrane protein in detergent-free aqueous solution. *Proc. Natl. Acad. Sci. U.S.A.* **102,** 8893–8898 CrossRef Medline
42. Champeil, P., Menguy, T., Tribet, C., Popot, J.-L., and Le Maire, M. (2000) Interaction of amphipols with sarcoplasmic reticulum Ca^{2+}-ATPase. *J. Biol. Chem.* **275,** 18623–18637 CrossRef Medline
43. Picard, M., Duval-Terrié, C., Dé, E., and Champeil, P. (2004) Stabilization of membranes upon interaction of amphipathic polymers with membrane proteins. *Protein Sci.* **13,** 3056–3058 CrossRef Medline
44. Watanabe, A., Kim, E., Burton-Smith, R. N., Tokutsu, R., and Minagawa, J. (2019) Amphipol-assisted purification method for the highly active and stable photosystem II supercomplex of *Chlamydomonas reinhardtii*. *FEBS Lett.* **593,** 1072–1079 CrossRef Medline
45. Burton-Smith, R. N., Watanabe, A., Tokutsu, R., Song, C., Murata, K., and Minagawa, J. (2019) Structural determination of the large photosystem II–light-harvesting complex II supercomplex of *Chlamydomonas reinhardtii* using nonionic amphipol. *J. Biol. Chem.* **294,** 15003–15013 CrossRef Medline
46. Sheng, X., Watanabe, A., Li, A., Kim, E., Song, C., Murata, K., Song, D., Minagawa, J., and Liu, Z. (2019) Structural insight into light harvesting for photosystem II in green algae. *Nat. Plants* **5,** 1320–1330 CrossRef Medline
47. Ware, M. A., Belgio, E., and Ruban, A. V. (2015) Comparison of the protective effectiveness of NPQ in *Arabidopsis* plants deficient in PsbS protein and zeaxanthin. *J. Exp. Bot.* **66,** 1259–1270 CrossRef Medline
48. Ware, M. A., Dall'Osto, L., and Ruban, A. V. (2016) An *in vivo* quantitative comparison of photoprotection in *Arabidopsis* xanthophyll mutants. *Front. Plant Sci.* **7,** 841 CrossRef Medline
49. Ilioaia, C., Duffy, C. D., Johnson, M. P., and Ruban, A. V. (2013) Changes in the energy transfer pathways within photosystem II antenna induced by xanthophyll cycle activity. *J. Phys. Chem. B* **117,** 5841–5847 CrossRef Medline
50. Johnson, M. P., Zia, A., Horton, P., and Ruban, A. V. (2010) Effect of xanthophyll composition on the chlorophyll excited state lifetime in plant leaves and isolated LHCII. *Chem. Phys.* **373,** 23–32 CrossRef
51. Ruban, A., and Horton, P. (1992) Mechanism of ΔpH-dependent dissipation of absorbed excitation energy by photosynthetic membranes: I. Spectroscopic analysis of isolated light-harvesting complexes. *Biochim. Biophys. Acta* **1102,** 30–38 CrossRef
52. Ruban, A., Rees, D., Pascal, A., and Horton, P. (1992) Mechanism of ΔpH-dependent dissipation of absorbed excitation energy by photosynthetic membranes: II. The relationship between LHCII aggregation *in vitro* and qE in isolated thylakoids. *Biochim. Biophys. Acta* **1102,** 39–44 CrossRef
53. Pandit, A., Shirzad-Wasei, N., Wlodarczyk, L. M., van Roon, H., Boekema, E. J., Dekker, J. P., and Willem, J. (2011) Assembly of the major light-harvesting complex II in lipid nanodiscs. *Biophys. J.* **101,** 2507–2515 CrossRef Medline
54. Petrou, K., Belgio, E., and Ruban, A. V. (2014) pH sensitivity of chlorophyll fluorescence quenching is determined by the detergent/protein ratio and the state of LHCII aggregation. *Biochim. Biophys. Acta* **1837,** 1533–1539 CrossRef Medline
55. Enriquez, M. M., Akhtar, P., Zhang, C., Garab, G., Lambrev, P. H., and Tan, H.-S. (2015) Energy transfer dynamics in trimers and aggregates of light-harvesting complex II probed by 2D electronic spectroscopy. *J. Chem. Phys.* **142,** 212432 CrossRef Medline
56. Magdaong, N. M., Enriquez, M. M., LaFountain, A. M., Rafka, L., and Frank, H. A. (2013) Effect of protein aggregation on the spectroscopic properties and excited state kinetics of the LHCII pigment–protein complex from green plants. *Photosynth. Res.* **118,** 259–276 CrossRef Medline
57. Chmeliov, J., Gelzinis, A., Franckevičius, M., Tutkus, M., Saccon, F., Ruban, A. V., and Valkunas, L. (2019) Aggregation-related nonphotochemical quenching in the photosynthetic membrane. *J. Phys. Chem. Lett.* **10,** 7340–7346 CrossRef Medline
58. Chmeliov, J., Gelzinis, A., Songaila, E., Augulis, R., Duffy, C. D., Ruban, A. V., and Valkunas, L. (2016) The nature of self-regulation in photosynthetic light-harvesting antenna. *Nat. Plants* **2,** 16045 CrossRef Medline
59. Miloslavina, Y., Wehner, A., Lambrev, P. H., Wientjes, E., Reus, M., Garab, G., Croce, R., and Holzwarth, A. R. (2008) Far-red fluorescence: a direct spectroscopic marker for LHCII oligomer formation in non-photochemical quenching. *FEBS Lett.* **582,** 3625–3631 CrossRef Medline
60. Nishimura, M., and Akazawa, T. (1975) Photosynthetic activities of spinach leaf protoplasts. *Plant Physiol.* **55,** 712–716 CrossRef Medline
61. Ostroumov, E. E., Götze, J. P., Reus, M., Lambrev, P. H., and Holzwarth, A. R. (2020) Characterization of fluorescent chlorophyll charge-transfer states as intermediates in the excited state quenching of light-harvesting complex II. *Photosynth. Res.* **144,** 171–193 CrossRef Medline
62. Johnson, M. P., and Ruban, A. V. (2009) Photoprotective energy dissipation in higher plants involves alteration of the excited state energy of the emitting chlorophyll(s) in the light harvesting antenna II (LHCII). *J. Biol. Chem.* **284,** 23592–23601 CrossRef Medline
63. Ruban, A. V., and Johnson, M. P. (2009) Dynamics of higher plant photosystem cross-section associated with state transitions. *Photosynth. Res.* **99,** 173–183 CrossRef Medline
64. Phillip, D., Ruban, A. V., Horton, P., Asato, A., and Young, A. J. (1996) Quenching of chlorophyll fluorescence in the major light-harvesting complex of photosystem II: a systematic study of the effect of carotenoid structure. *Proc. Natl. Acad. Sci. U.S.A.* **93,** 1492–1497 CrossRef Medline
65. Ruban, A. V., Phillip, D., Young, A. J., and Horton, P. (1997) Carotenoid-dependent oligomerization of the major chlorophyll a/b light harvesting complex of photosystem II of plants. *Biochemistry* **36,** 7855–7859 CrossRef Medline
66. Kim, E., Watanabe, A., Duffy, C. D. P., Ruban, A. V., and Minagawa, J. (2020) Multimeric and monomeric photosystem II supercomplexes represent structural adaptations to low- and high-light conditions. *J. Biol. Chem.* **295,** 14537–14545 CrossRef Medline
67. Popot, J.-L., Berry, E. A., Charvolin, D., Creuzenet, C., Ebel, C., Engelman, D. M., Flötenmeyer, M., Giusti, F., Gohon, Y., Hong, Q., Lakey, J. H., Leonard, K., Shuman, H. A., Timmins, P., Warschawski, D. E., *et al.* (2003) Amphipols: polymeric surfactants for membrane biology research. *Cell. Mol. Life Sci.* **60,** 1559–1574 CrossRef Medline
68. Tribet, C., Diab, C., Dahmane, T., Zoonens, M., Popot, J.-L., and Winnik, F. M. (2009) Thermodynamic characterization of the exchange of detergents and amphipols at the surfaces of integral membrane proteins. *Langmuir* **25,** 12623–12634 CrossRef Medline
69. Zoonens, M., Giusti, F., Zito, F., and Popot, J.-L. (2007) Dynamics of membrane protein/amphipol association studied by Förster resonance energy transfer: implications for *in vitro* studies of amphipol-stabilized membrane proteins. *Biochemistry* **46,** 10392–10404 CrossRef Medline

70. Martinez, K. L., Gohon, Y., Corringer, P.-J., Tribet, C., Mérola, F., Changeux, J.-P., and Popot, J.-L. (2002) Allosteric transitions of Torpedo acetylcholine receptor in lipids, detergent and amphipols: molecular interactions *vs.* physical constraints. *FEBS Lett.* **528,** 251–256 CrossRef Medline
71. Noctor, G., Rees, D., Young, A., and Horton, P. (1991) The relationship between zeaxanthin, energy-dependent quenching of chlorophyll fluorescence, and trans-thylakoid pH gradient in isolated chloroplasts. *Biochim. Biophys. Acta* **1057,** 320–330 CrossRef
72. Johnson, M. P., Pérez-Bueno, M. L., Zia, A., Horton, P., and Ruban, A. V. (2009) The zeaxanthin-independent and zeaxanthin-dependent qE components of nonphotochemical quenching involve common conformational changes within the photosystem II antenna in *Arabidopsis*. *Plant Physiol.* **149,** 1061–1075 CrossRef Medline
73. Ruban, A., Rees, D., Noctor, G., Young, A., and Horton, P. (1991) Long-wavelength chlorophyll species are associated with amplification of high-energy-state excitation quenching in higher plants. *Biochim. Biophys. Acta* **1059,** 355–360 CrossRef
74. Pascal, A. A., Liu, Z., Broess, K., van Oort, B., van Amerongen, H., Wang, C., Horton, P., Robert, B., Chang, W., and Ruban, A. (2005) Molecular basis of photoprotection and control of photosynthetic light-harvesting. *Nature* **436,** 134–137 CrossRef Medline

A novel method produces native light-harvesting complex II aggregates from the photosynthetic membrane revealing their role in nonphotochemical quenching

Mahendra K. Shukla, Akimasa Watanabe, Sam Wilson, Vasco Giovagnetti, Ece Imam Moustafa, Jun Minagawa and Alexander V. Ruban

J. Biol. Chem. 2020, 295:17816-17826.
doi: 10.1074/jbc.RA120.016181 originally published online October 20, 2020

A novel method produces native LHCII aggregates from the photosynthetic membrane revealing their role in non-photochemical quenching (JBC/2020/015695) by M.K. Shukla, A. Watanabe, S. Wilson, V. Giovagnetti, E. Imam Moustafa, J. Minagawa, A.V. Ruban

Supplementary information.

Figure S1. SDS-PAGE of thylakoid membranes isolated from *NoM* lincomycin-treated plants and wild type *Arabidopsis thaliana*. LHCII trimers, PSII and PSI core proteins are indicated. Proteins were visualised using Coomassie staining. 1 µg chlorophyll of thylakoid membranes was loaded onto each lane.

Figure S2. Isolation of LHCII antenna complexes from photosynthetic membranes of *NoM* plants treated with lincomycin, by sucrose density gradients. Different isolation procedures are compared: 0.5% α-DM (**A**), 0.3% α-DM + 0.5% digitonin **(B)** and 0.3% α-DM + 0.5% digitonin followed by amphipol A8-35 replacement of detergents (**C**).

Figure S3. Identification of the bands isolated by sucrose density gradients (from Figure 1A). SDS-PAGE of violaxanthin-enriched samples, under dark (**A**) and NPQ state (**B**). Two gels were run in parallel for each condition (dark and NPQ), one was used to visualize the protein composition (Coomassie blue staining), while the second gel was used for western blot analysis. For clarity purposes, only the major pigmeted bands collected from sucrose density gradients are labelled (i.e. LHCII tr., PSI/LHCI/LHCII and LHCII aggregates). In the SDS-PAGE gel, the localisation of PSII and PSI core, and LHCII, proteins is indicated.

Figure S4. Identification of the bands isolated by sucrose density gradients (from Figure 1B). SDS-PAGE of zeaxanthin-enriched samples, under dark (**A**) and NPQ state (**B**). Two gels were run in parallel for each condition (dark and NPQ), one was used to visualize the protein composition (Coomassie blue staining), while the second gel it was used for western blot analysis. For clarity purposes, only the major pigmeted bands collected from sucrose density gradients are labelled (i.e. LHCII tr., PSI/LHCI/LHCII and LHCII aggregates). In the SDS-PAGE gel, the localisation of PSII and PSI core, and LHCII, proteins is indicated.

Figure S5. Isolation of the trimeric and aggregated form of LHCII (LHCII tr. and LHCII ag.) from solubilised photosynthetic membranes by using sucrose density gradient. Zeaxanthin-enriched *NoM* thylakoids devoid of photosystem cores, under dark and NPQ states, are compared. The NPQ state was fixed by adding 0.5 mM dithiobis[succinimidyl propionate] (DSP).

Figure S1. Shukla et al.

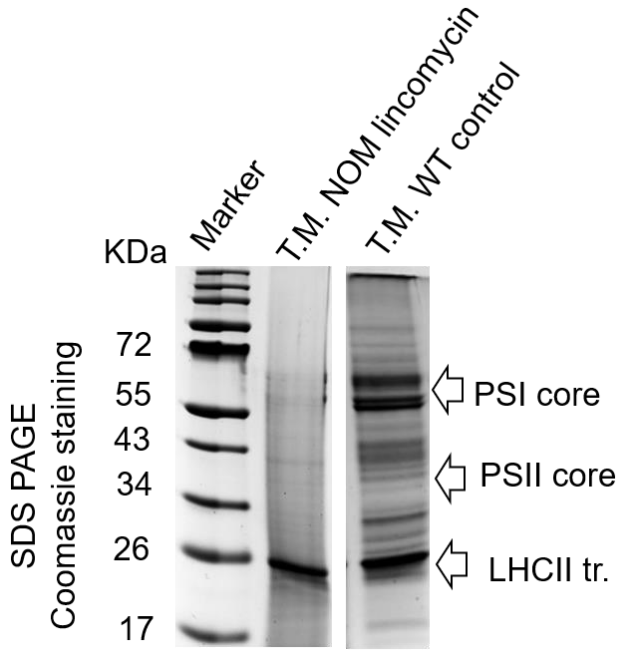

Figure S2. Shukla et al.

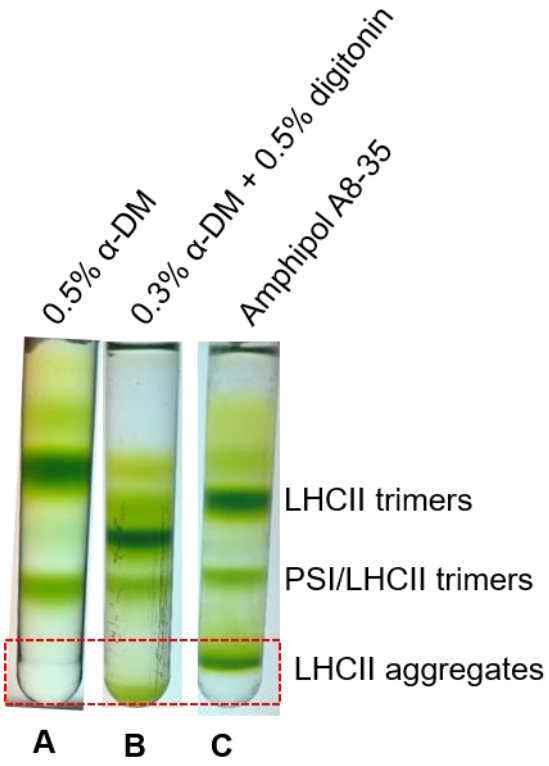

Figure S3. Shukla et al.

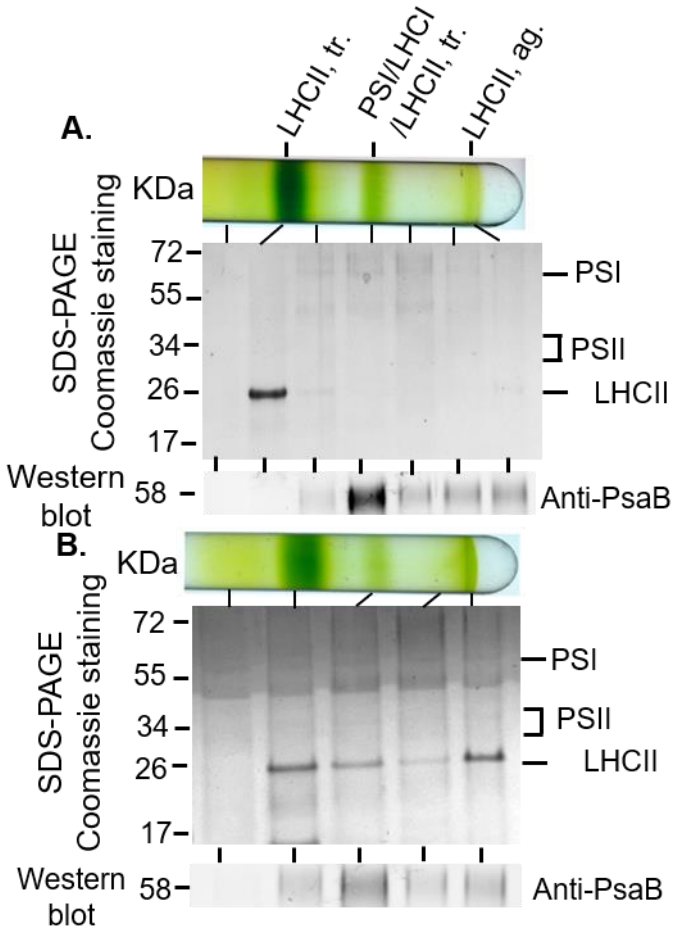

Figure S4. Shukla et al.

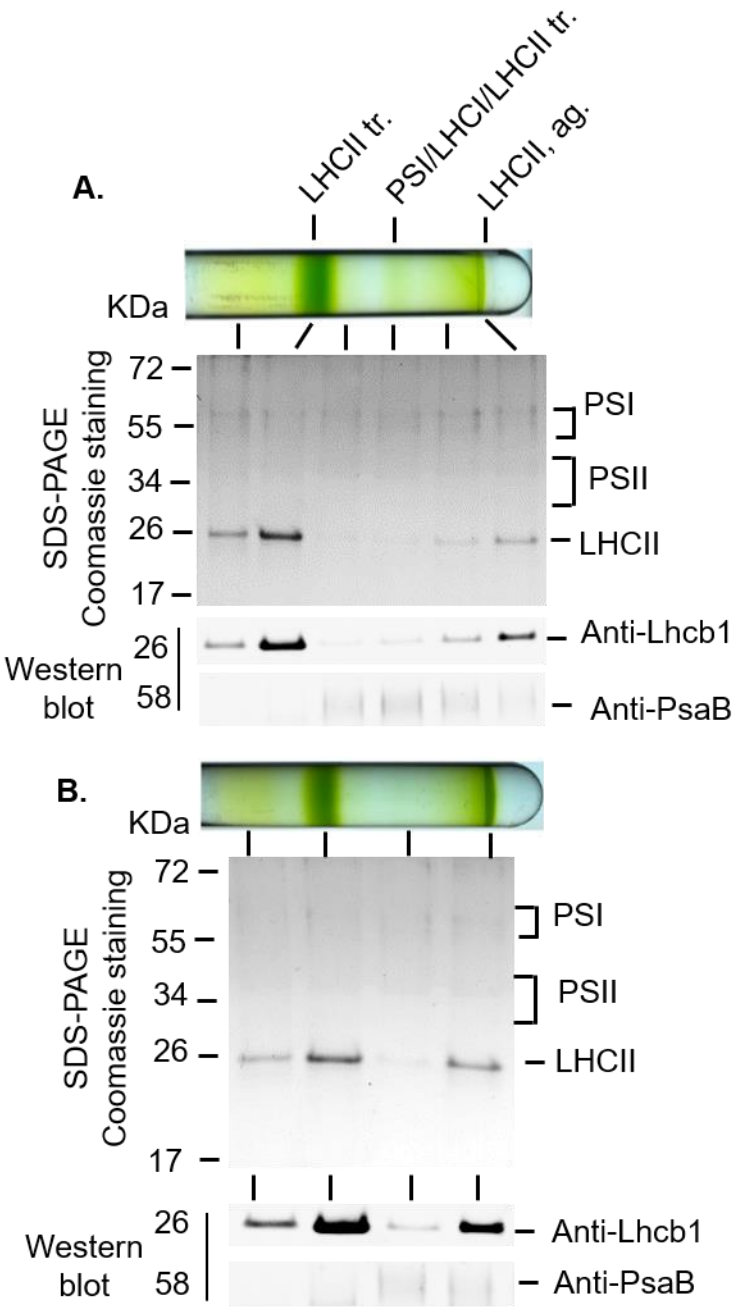

Figure S5. Shukla et al.

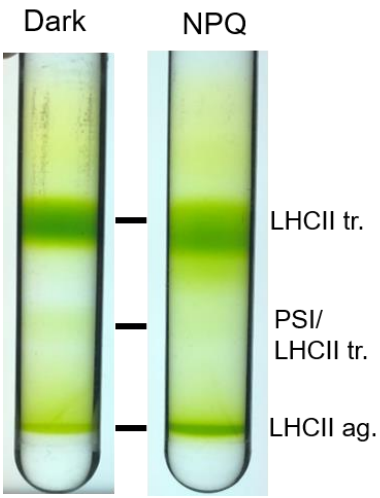

Table S1. Lifetime components of the trimeric and aggregated LHCII antenna in NPQ state. The pigment-protein complexes measured here were obtained from zeaxanthin-enriched photosynthetic membrane (Figure 1B, NPQ state). Fluorescence lifetime decay kinetics are shown in Figure 3. Fluorescence lifetime measurements were performed on two independent replicates.

Table S2. Relative chlorophyll contribution of LHCII trimers and aggregates in violaxanthin-enriched thylakoid membranes. Samples were isolated by sucrose density gradient

unltracentrifugation (see Figure 1). Dark and NPQ states are compared. Experiments were performed on two independent replicates.

Table S3. Relative chlorophyll contribution of LHCII trimers and aggregates in zeaxanthin-enriched thylakoid membranes. Samples were isolated by sucrose density gradient unltracentrifugation (see Figure 1). Dark and NPQ states are compared. Experiments were performed on three independent replicates.

Table S1

Sucrose density bands	Intensity weighted t_1 (ns), %	t_2 (ns), %	t_3 (ns), %	Average life time (ns)

Zea (NPQ), LHCII tr.	0.335 ± 0.03 ns, 3.5 ± 1.4%	2.06 ± 0.049 ns, 20 ± 4%	3.83 ± 0.03 ns, 75 ± 5.5 %	3.36 ± 0.06 ns
Zea (NPQ), LHCII ag.	0.18 ± 0.05 ns, 41 ± 5%	0.54 ± 0.22 ns, 47 ± 8%	2.8 ± 0.26 ns, 11.5 ± 3.5%	0.61 ± 0.08 ns

Table S2

Sucrose density gradient (Violaxanthin)	**LHCII trimer (Chl%)**	**Average Chl%**	**LHCII aggregate (Chl%)**	**Average Chl%**

Viol (dark) r_1	92.77	91.6 ± 1.65	7.22	8.39 ± 1.65
Viol (dark) r_2	90.43		9.56	
Viol (NPQ) r_1	86.66	84.45 ± 3.12	13.33	15.54 ± 3.12
Viol (NPQ) r_2	82.24		17.75	

Table S3

Sucrose density gradient (Zeaxanthin)	**LHCII trimer (Chl%)**	**Average Chl%**	**LHCII aggregate (Chl%)**	**Average Chl%**
Zea (dark) r_1	86.22	84.053 ± 2.273	13.77	15.94 ± 2.273

Zea (dark) r_2	81.68		18.31	
Zea (dark) r_3	84.24		15.75	
Zea (NPQ) r_1	63.55	66.14 ± 2.27	36.44	33.85 ± 2.27
Zea (NPQ) r_2	67.79		32.2	
Zea (NPQ) r_3	67.07		32.9	